RSC Advances

ROYAL SOCIETY OF CHEMISTRY

www.rsc.org/advances

Journal Name

RSCPublishing

ARTICLE

Magnetic Anisotropy Induced in NiCo Granular Nanostructures by ZnO Nanorods Deposited on A Polymer Substrate

Yi Chen,[a] Xiaoxuan Guo,[b] Wai Hei Tse, [a] Tsun-Kong Sham[b] and Jin Zhang[a*]

Cite this: DOI: 10.1039/x0xx00000x

Received 00th January 2012,
Accepted 00th January 2012

DOI: 10.1039/x0xx00000x

www.rsc.org/

Hetero-nanostructures made of NiCo and ZnO nanostructures have been deposited on a polymer substrate through a two-step method. First ZnO nanorod (NR) array was grown on polydimethylsiloxane (PDMS) substrate by a hydrothermal method. NiCo granular nanostructures were then deposited on ZnO nanorod array through the electroless polyol process with precursors of Ni complex and Co complex in the mole ratio of 50:50. The effect of deposition time (t) on the structure and properties of the hetero-nanostructures have been studied. Ni-rich nanostructures are observed when *t* <30 min. With t increasing, the atomic ratio (at. %) of Ni to Co is approaching to 50:50. In addition, a magnetic field (10 KOe) was applied on the hetero-nanostructures, which was parallel (//) and perpendicular (⊥) to the ZnO nanorods, respectively. The magnetization (*Ms*) of the NiCo nanostructures deposited on ZnO nanorods when t = 60 min is measured at 93.4 emu/g. The results of magnetic measurement and X-ray absorption near edge structure spectroscopy (XANES) suggest that the slightly lower magnetizations of the hetereo-nanostructures may be caused by the oxidation of Co and Ni on the surface of the granular films. The values of squareness ratio (*Mr/Ms*) of the hetero-nanostructures with *t* are far below 0.5. Moreover, the coercivity (*Hc*) values of the hetero-nanostructures measured in the direction perpendicular to the ZnO nanorods is higher than that in the parallel direction. Therefore, the deposited NiCo granular nanostructures are perpendicular to the plane of PDMS substrate, and show the perpendicular magnetic anisotropy. These results clearly demonstrate that the rod-shaped non-magnetic nanomaterials can significantly affect the magnetic anisotropy of the hetero-nanostructures.

INTRODUCTION

Magnetic and non-magnetic hetero-nanostructures show distinguished properties, and have been applied in various devices, e.g. non-volatile magnetic random access memory (MRAM) based on magnetic tunnel junctions, sensors based on giant magnetoresistance (GMR). Control the interface of magnetic and non-magnetic materials is a challenge to precisely gain the desired properties.

Nickel (Ni) and cobalt (Co) nanostructures have been extensively studied due to their magnetic properties. Incorporation of Ni-, and Co- nanostructures with semiconductors has shown enhanced catalytic activity and improved corrosion resistance, and could be applied in new spintronic devices.[1] On the other hand, zinc oxide (ZnO) is a wide-band-gap semiconductor with band gap energy of 3.37 eV and a large excitation binding energy of 60 meV. One-dimensional zinc oxide (ZnO) nanostructures including nanorods and nanowires have been considered as the most efficient potential material of light emitting diode (LED), transistor, solar cell and Schottky diode due to its electrical, optical, and piezoelectric properties.[2-5]

Recently, one-dimensional ZnO nanostructures incorporating with transitional metals, e.g. Ni and Co, have shown interesting magnetic properties depending on different processing methods, such as chemical vapor deposition (CVD), core/shell formation, sputtering, and electrochemical deposition.[6-8] Unfortunately, these methods normally require expensive deposition systems and complex processes. Compared to these vacuum-involved deposition processes, chemical solution methods may provide an alternative solution to develop magnetic hetero-nanostructures. For instance, Dr. Huang and his co-work developed electrochemical method to deposit Ni-doped ZnO nanocomposites on metallic substrates.[9-10] In addition, our previous studies indicate that hybrid metallic nanostructures can be deposited on metal and ceramic substrates through an electroless polyol process, which is a reductive regent-free, low temperature process.[11-12].

To develop a magnetic and non-magnetic hetero-nanostructures on polymer substrates with more flexible mechanical properties, and to further understand the effect of the interface between magnetic and non-magnetic nanostructures on magnetic properties, a two-step process has been developed for fabricating magnetic metal/ZnO nanocomposite on a flexible substrate made by polymers. First aligned ZnO nanorod (NR) array were grown on polydimethylsiloxane (PDMS) substrate. Subsequently, the NiCo granular film was deposited on the ZnO NR array by an electroless polyol method. The effect of deposition time (*t*) on the microstructures and magnetic properties of NiCo-ZnO hertero-nanostructures have been discussed in this paper.

EXPRIMENTAL DETAILS

Well-aligned ZnO nanorod (NR) array was grown on flexible substrate through modifying previous reported method.[13-14] Briefly, zinc acetate dehydrate (0.01 M) was dissolved in 100 mL ethanol as a seed solution. The seed solution was dropped on a PDMS substrate repeatedly followed a heat treatment at 100 ^{0}C for 1 hour (h). The ZnO seeds coated PDMS film was then immersed in the mixed solution of zinc nitrate hexahydrate (0.025 M) and hexamethylenetetramine (HMTA 0.025 M) in 200 mL of distilled deionized water. After heated at 90 ^{0}C for 3 h, the ZnO nanorod array was grown on the PDMS as shown in Scheme 1. Samples were rinsed by distilled deionized water and dried at room temperature.

Equimolar nickel (II) acetate tetrahydrate and cobalt (II) acetate tetrahydrate were dissolved in 200 ml of ethylene glycol (EG). The mixture was heated at 194 ^{0}C with refluxing.[11] Our previous studies indicate that the growth of metallic films produced by polyol process nonlinearly depends on the deposition time (*t*),[11-12] e.g. the growth of film increases dramatically when t < 30 min, whereas the thickness and weight of films increas slowly when 30 min< t <60 min, and no further growth can be observed when t > 60 min. Therefore, the

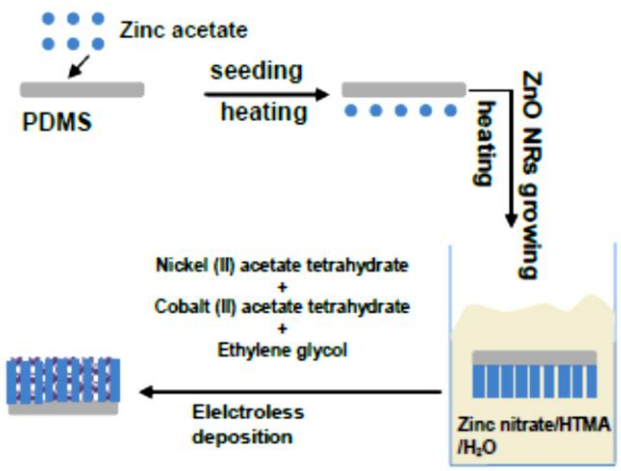

Scheme 1. Illustration of the two-step method for fabricating NiCo nanostructures coated ZnO nanorod array on PDMS.

produced ZnO NR array coated on PDMS was suspended into the solution. NiCo granular films were deposited on ZnO NR arrays when the deposition time (*t*) is 10 min, 30 min, and 60 min, respectively. Here, the deposited samples are denoted as NiCo-ZnO-10, NiCo-ZnO-30 and NiCo-ZnO-60. All substrates have the same dimension (3x3 cm^2). An illustration is displayed below to show the fabrication process of NiCo-ZnO hetero-nanostructures.

The morphology of the aligned ZnO NR array was studied by the Scanning Electron Microscopy (SEM, Hitachi 3400S). Energy Dispersive X-ray Spectroscopy (EDX) was used to find out the distribution of Ni and Co on the ZnO NR array. X-ray diffraction (XRD) was carried out (Rigaku rotating-anode X-ray diffractmeter with Co-Ka radiation) to study the crystal structures of the hybrid nanocomposites. In addition, magnetic properties of the NiCo-ZnO hetero-nanostructures were measured by using vibrating sample magnetometer (VSM, LakeShore 7407, moment measure range: 10^{-7}-10^3 emu; field accuracy: ±0.05% full scale). All the magnetization measurements were carried out at room temperature under a maximum field of 10 kOe. The field was applied in the direction parallel (//) or perpendicular (⊥) to the ZnO NR as shown in the Scheme 2.

The weights of all the films were measured by weighing the

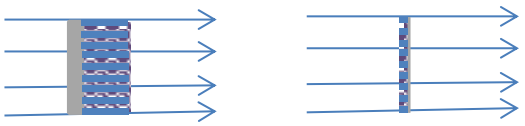

Magnetic field parallel (//) to ZnO nanorod array

Magnetic Field perpendicular (⊥) to ZnO nanorod array which points out of the paper)

Scheme 2. The two direction of magnetic measurements. (left) Magnetic field parallel to ZnO nanorods; (right) Magnetic field perpendicular to ZnO nanorods.

substrate before and after the film deposition using a balance with ±0.0005% of accuracy.

$$g_{NiCo\ film} = g_{ZnO+PDMS+NiCo\ film} - g_{ZnO+PDMS} . \quad (1)$$

Film growth was studied by investigating the development of morphology, structure, composition and microstructure including crystallite size, strain, and film thickness by different kinds of techniques.

To study the surface of the hybrid films, the Ni and Co K-edge X-ray absorption near edge structure spectroscopy (XANES) experiments were conducted at Soft X-ray Microcharacterization Beamline (SXRMB) in Canadian Light Source (CLS). The samples were mounted on the copper plate in a vacuum chamber (around 10^{-8} Torr). XANES spectra were collected in total electron yield (TEY). TEY measured all the electrons ejected from the specimens, including photoelectrons, Auger electrons and secondary electrons. TEY mode experimentally monitored the neutralization current to ground, and extremely surface sensitive since the electron escape depth is very short.

RESULTS AND DISCUSSION

To grow ZnO NR array on PDMS, hexamethylenetetramine (HMTA) is used to provide OH^- anions which helps to form $Zn(OH)_4^{2-}$,[13] meanwhile, the ZnO nanorods can be dehydrated by the intermediates. This fast and simple synthesis method also exhibit good control over the ZnO nanomaterial morphologies by changing the reaction condition such as reaction temperature, pH and time duration.[14-16] SEM surface micrographs for the bare ZnO NR array prepared on PDMS substrate are shown in Figure 1. Figure 1a is the SEM micrographs of the vertically aligned ZnO rod grown on PDMS, and individual ZnO nanorod. The average diameter of ZnO nanorods is estimated at 160±5 nm with a length of 2±0.5 µm. Figure 1b presents high magnification ZnO NR SEM micrograph in which individual ZnO NR has hexagonal-shaped

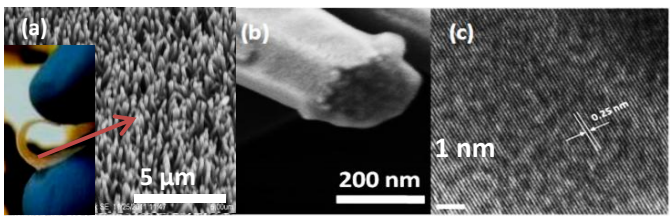

Figure 1. Electron microscope micrographs of ZnO nanorods. (a) SEM micrograph of ZnO NR array on PDMS. The small inset shows the foldable sample. (b) SEM micrograph of ZnO NR with 200 nm in diameter. (c) High resolutionREM micrograph of ZnO NR.

structure. HRTEM of ZnO NR lattice image (Figure 1c) indicates the ZnO NRs are highly crystalline with a lattice spacing of 0.25 nm which corresponds to the (0002) planes in the ZnO crystal lattice.[17-18]

In the polymer process, ethylene glycol is used as reductive regent to produce fine metallic nanoparticles. Our previous work successfully indicates the metallic thin film can be deposited on metal and ceramic substrates through the polyol process.[10-11] Here, bi-element NiCo nanostructures were deposited on ZnO NR array grown on the flexible polymer substrate, PDMS, through the polyol process. Figure 2 shows the cross-sectional SEM micrographs of ZnO nanorod array on PDMS before and after the deposition of NiCo nanostructures when t = 15 min. Figure 2b clearly shows the NiCo nanostructures deposited on the sidewall of ZnO nanorods with 2±0.5 µm in length, and the growth texture of NiCo granular

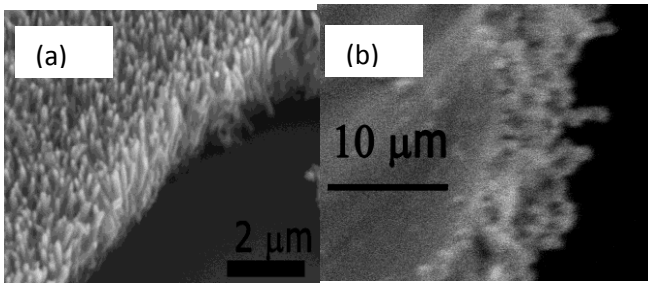

Figure 2. Cross-sectional SEM micrographs (a) ZnO nanorods grown on PDMS (b) NiCo gradular nanostructures deposited on ZnO nanorod arrays grown on PDMS.

film (above the ZnO nanorod array) prefers to be normal to the PDMS substrate, which is influenced by the ZnO nanorods vertically grown on PDMS. The thickness of NiCo-ZnO increases from 6±0.8 µm to 11±1.5 µm when t increases from 15 min to 60 min. Figure 3 shows the morphologies of NiCo-ZnO with different deposition time, t = 10min, 30min, and 60min, respectively. Clearly, the surface of NiCo-ZnO show granular nanostructures which are NiCo coatings. The surface compositions of the hetero-nanostructures were identified by EDX data. Only Zn, O, Co and Ni peaks can be observed in EDX spectrum (Figure 3d). The correlation between the deposition time and surface compositions (atomic ratio: at.%) is listed in Table 1. The Ni-rich (58.3±1.25 at.%) composition can be found in NiCo-ZnO-10. Co at.% increases from 41.7±1.25 at.% to 50.2±1.25 at.% when t increases from 10 min to 60 min. It indicates that it takes longer time to deposit the reduced Co in polyol process due to its higher reduction potential (-0.28 V) compared to Ni (-0.257 V).[19]

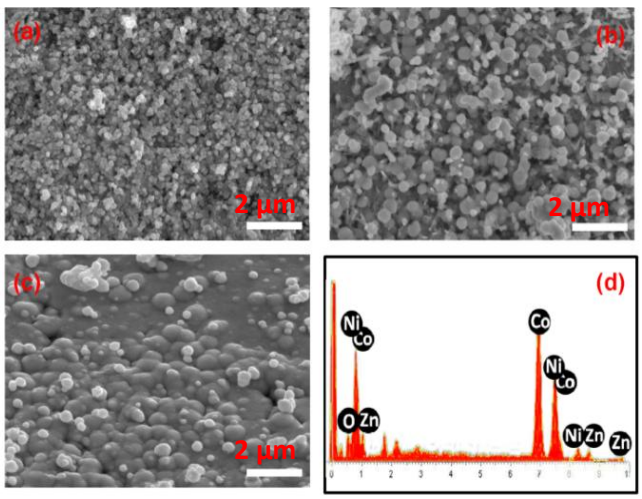

Figure 3. (a) SEM micrograph of NiCo-ZnO-10. (b) SEM micrograph of NiCo-ZnO-30 (c) SEM micrograph of NiCo-ZnO-60. (d) EDX spectrum of NiCo-ZnO-60.

Table 1. Atomic ratio of the NiCo nanostructures coated on ZnO NR array

Samples	Thickness of NiCo-ZnO (µm)	Ni (at.%)	Co (at.%)
NiCo-ZnO-10	6±0.8	58.3±1.25	41.7±1.25
NiCo-ZnO-30	9±1.0	52.6±1.25	47.4±1.25
NiCo-ZnO-60	11±1.5	49.8±1.25	50.2±1.25

In addition, XRD was carried out to further study the structure of NiCo-ZnO hetero-nanostructures. In Figure 4, the diffraction patterns clearly show the preferential growth along the (002) plane in the wurtzite structure of ZnO (JCPDS no. 36-1451), which indicates the highly crystalline structure with along c-axis growth orientation of hexagonal structure.[7] When t =10 min, two new weak peaks can be observed as shown in Figure 4, which match well with the face-centred cubic (fcc) of

Ni/Co structures. It is hard to identify the fcc Ni (JCPDS no. 15-0806) and fcc Co (01-1260) peaks due to their similar crystal structures. We therefore study the long-range order of the hetero-nanostructures through X-ray absorption near edge structure spectroscopy (XANES), which is discussed later. With the deposition time increasing, the intensity of the diffraction peaks of NiCo increases. There is no other characteristic peak of the impurities. Meanwhile, Scherrer equation is applied to estimate the crystallite size of the NiCo nanocomposite;[20-21]

$$D = \frac{K\lambda}{\beta \cos\theta}$$

where D is the crystallite size, K is the constant on crystallite shape (0.89), λ is the X-ray wavelength, β is the full width at half max (FWHM) of (111) diffraction peak, and θ is the Bragg angle. The average crystalline size of CoNi coated on ZnO NR arrays is estimated at 67.8±5 nm, which is independent to *t*.

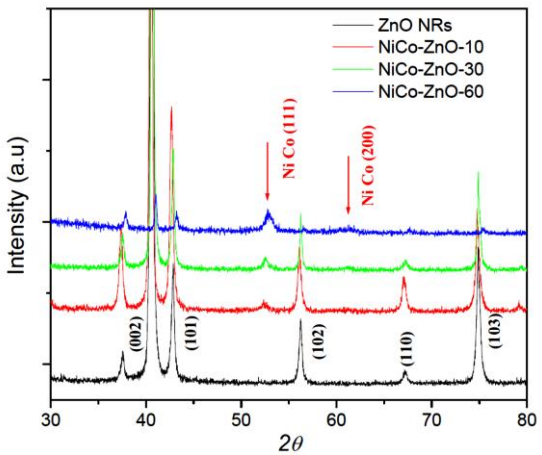

Figure 4. XRD profiles of NiCo granular film coated on ZnO NR array with *t*.

The magnetic hysteresis loops of the NiCo-ZnO hetero-nanostructures were measured at 300 K with the applied field, -10 kOe < H <10 kOe. The background of PDMS substrate has been subtracted. The bare ZnO NR array shows diamagnetic behaviour while NiCo-ZnO hetero-nanostructures have strong ferromagnetic features at 300 K. In addition, the value of saturation magnetization (M_s) of NiCo-ZnO hetero-nanostructures increases from 86.36 emu/g to 95.39 emu/g when *t* increases from 10 min to 60 min as shown in Table 2. It corresponds to the increasing atomic ratio of Co in the hetero-nanostructures with *t* (i.e. Co at.% from 41.7±1.25 to 50.2±1.25). Our previous studies on polyol process indicate that the thickness and weight of thin films have non-linear relationships to the deposition time.

In most cases, both of the thickness and weight increase dramatically when *t* <30 min; the deposition films grow slowly when *t* >30 min; there is no more growth after *t* = 60 min. The most interesting results are related to the magnetic anisotropy of the NiCo-ZnO hetero-nanostructures. All samples with increasing *t* show clear magnetic anisotropy under the field direction (parallel and perpendicular to the nanorod array). Figure 5 shows the hysteresis loops of NiCo-ZnO-60 when the applied field is parallel to the ZnO NR array and perpendicular to the ZnO NR array, respectively. The values of squareness ratio (*Mr/Ms*) and coercivity (*Hc*) of the samples with two different field directions are also listed in Table 2. The squareness ratio (*Mr/Ms*) is dominated by the uniaxial anisotropy, e.g. *Mr/Ms* =0.5 when single domain particles are randomly oriented. Here, all samples have very small squareness ration, which indicates the magnetic domains are oriented. Furthermore, higher *Hc* of samples under a magnetic field perpendicular to the ZnO NR array indicate that the deposited NiCo are oriented to the opposite direction, i.e. perpendicular to the plane of PDMS substrate. In addition, the anisotropy field (H_K) of the nanostructured hetero-nanostructures decrease from 10.7 KOe to 8.6 KOe when *t* increases from 10 min to 60 min. To thin films, the magnetic dipolar interaction (*Kv*) is a major source for the magnetic anisotropy. Due to its long-range character, the dipolar

Table 2. Magnetic saturation (*Ms*), squareness ratio (*Mr/Ms*), and Coercivity (H_c) of NiCo nanostructured granular films coated on ZnO nanorods.

Field Parallel(//) to ZnO nanorods	*Ms* (emu/g)	M_r/M_s	*Hc* (Oe)
NiCo-ZnO-10	85	0.15	60
NiCo-ZnO-30	92.3	0.18	86
NiCo-ZnO-60	93.4	0.18	97
Field perpendicular (⊥) to ZnOnanorods	*Ms* (emu/g)	M_r/M_s	*Hc* (Oe)
NiCo-ZnO-10	85	0.07	116
NiCo-ZnO-30	92.3	0.08	130
NiCo-ZnO-60	93.4	0.11	138

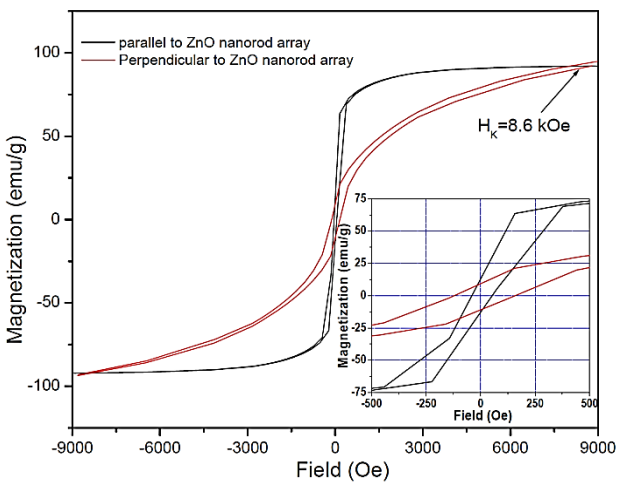

Figure 5. Hysteresis loops of NiCo-ZnO-60 in two directions. Small inset figure indicate the higher coercivity of NiCo-ZnO-60 when magnetic field is perpendicular to the nanorods.

interaction generally results in a contribution to the anisotropy which depends on the shape of specimen.[22-23] Consequently, the magnetic anisotropy of NiCo-ZnO heterostructures is clearly significant influenced by the ZnO nanorods.

The *Ms* of bulk fcc Ni and fcc Co are 55, 168 emu/g at 300 K, respectively. It is noted that the Ms (93.4 emu/g) of NiCo-ZnO-60 is lower than that (111.7 emu/g) of bulk $Ni_{50}Co_{50}$. This could be caused by the oxidation on the surface of NiCo granular film produced by polyol process.[24] In order to determine the oxidation state of Co and Ni at the surface of the hetero-nanostructures, the X-ray absorption near edge structure

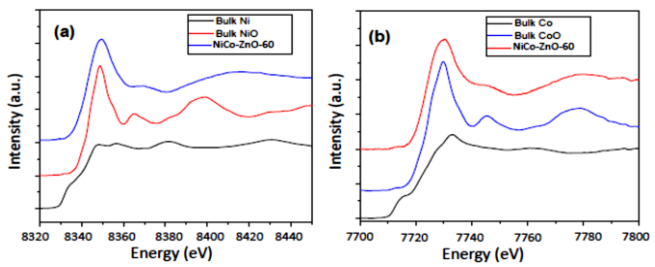

Figure 6. XANES spectra of the surface of NiCo-ZnO-60. (a) Ni K-edge XANES (b) Co K-edge XANES.

(XANES) spectroscopy is applied to study the surface of specimens. TEY spectra of NiCo–ZnO-60 were collected as shown in Figure 6. The probing depth of secondary electrons is around 20 Å, which makes the TEY-detection surface sensitive.[25] Figure 6(a) shows the Ni K-edge XANES of of NiCo-ZnO-60 sample, bulk Ni, and bulk NiO. The main resonance located around 8343 eV, is due to the electron transitions from 1s to 4p orbital,[26] while the shoulder peak around 8370 eV and the following broad peak around 8415 eV are arose from multiple scattering. In Figure 6(a), we found out that the TEY spectrum of NiCo-ZnO-60 is very close to that of NiO curve. Similar to the case of Co, there are no discernible differences can be observed between TEY and FY spectra of NiCo-ZnO-60 at Co K-edge as well. The Co K-edge XANES is very similar to the spectrum of CoO (Figure 6(b)).

CONCLUSION

We successfully developed a two-step method for coating NiCo nanostructured granular films on well-aligned ZnO NR array which is deposited on a flexible substrate, PDMS. The ZnO NRs are highly crystallite structures with 2.5 μm in height and 200 nm in diameter. Polyol process is able to be used to deposite metallic nanostructures on ZnO nanorods. The growth of the hetero-nanostructured NiCo-ZnO non-linearly depend on t. Ni-rich film is observed when $t < 30$ min, the atomic ratio of Ni and Co approaches to 50:50 when t is 60 min. The most interesting result is, the magnetic anisotropy of the hertero-nanostructured NiCo-ZnO is significant influenced by the shape of the non-magnetic ZnO nanorods. The perpendicular magnetic anisotropy of the NiCo-ZnO granular nanostructures on PDMS have a potential to be applied in high-density magnetic recording media, which normally require small crystalline size, and perpendicular magnetic anisotropy. Furthermore, our developed two-step method has advantages for fabricating magnetic-nonmagnetic hetero-nanostructures on polymer substrates with a simple and inexpensive manner. Polymer substrates may allow magnetic devices having light-weight and flexible mechanic properties.

Acknowledgements

This work was supported by the Grants (to Jin Zhang) of the Natural Sciences and Engineering Research Council of Canada (NSERC) and Canada Innovation Fund-Leader of innovation.

Notes and references

[a] Department of Chemical and Biochemical Engineering, University of Western Ontario, London, ON N6A 5B9 Canada
[b] The Chemistry Department, University of Western Ontario, London, ON N6A 5B9 Canada

1. S. G. J. Heijmand and H. N. Stein, *Langmuir*, 1995, **11**, 422.
2. Z. L. Wang, J. Song, *Science* **2006**, 312, 242.
3. P. X. Gao and Z. L. Wang, *J. Appl. Phys*., 2005, **97**, 044304.
4. S. J. Jiao, Z. Z. Zhang, Y. M. Lu, D. Z. Shen, B. Yao, J. Y. Zhang, B. H. Li, D. X. Zhao, X. W. Fan, and Z. K. Tang, *App. Phys. Lett*., 2006, **88**, 031911.
5. L. Li, T. Zhai, Y. Bando, and D. Golberg, *Nano Energy*, 2012, **1**, 91.
6. S. W. Jung, W. I. Park, G. C. Yi, and M. Y. Kim, *Adv. Mater*., 2003, **15**, 1358.
7. Y. J. Chen, F. Zhang, G. G. Zhao, X.Y. Fang, H. B. Jin, P. Gao, C. L. Zhu, M. S. Cao, and G. Xiao, *J. Phys. Chem. C*, 2010, **114**, 9239.
8. S. Zhang, Y. Shen, H. Fang, S. Xu, J. Song, and Z. L. Wang, *J. Mater. Chem*., 2010, **20**, 10606.
9. X. H. Huang, Z. Y. Zhan, K. P. Pramoda, C. Zhang, L. X. Zheng and S. J. Chua, *CrystEngComm*, 2012, **14**, 5163.
10. X. H. Huang, G. H. Li, B. Q. Cao, M. Wang, and C. Y. Ha, *J. Phys. Chem. C* 2009, **113**, 4381.
11. J. Zhang and G. M. Chow, *J. Applied Physics*, 2000, **88**, 2125.
12. J. Zhang and L. Chen, *Mater. Lett*., 2011, **65**, 2944.
13. R. Wahab, Y. S. Kim, K. Lee, and H.S. Shin, *J. Mater. Sci*., 2010, **45**, 2967.
14. Q. Li, V. Kumar, Y. Li, H. Zhang, T. J. Marks, and R. P. H. Chang, *Chem. Mater*., 2005, **17**, 1001.
15. W. Y. Wu, W. Y. Kung, and J. M. Ting, *J. Am. Ceram. Soc*., 2011, **94**, 699.
16. J. Zhang, Sun, Yin, Su, Liao, and Yan, *Chem. Mater*., 2002, **14**, 4172.
17. A. Manekkathodi, M.Y. Lu, C. W. Wang, and L. J. Chen, *Adv. Mater*., 2010, **22**, 4059.
18. Y. F. Yuan, J. P. Tu, S. Y. Guo, J. B. Wu, M. Ma, J. L. Yang, and X. L. Wang, *Appl. Surf. Sci*., 2008, **254**, 5080.
19. R. B. Brownlee, R. W. Fuller, and J. E. Whitsit, in "Elements of Chemistry"; Allyn and Bacon: Boston, Massachusetts, 1959; p 151.
20. J. I. Langford and A. J. C. Wilson, *J. Appl. Cryst.* 1978, **11** 102.
21. X. H. Huang, Z. Y. Zhan, X. Wang, Z. Zhang, G. Z. Xing, D. L. Guo, D. P. Leusink, L. X. Zheng, and T. Wu, *Appl. Phys. Lett*. 2010, **97**: 203112.
22. J. W. Matthews and J. L. Crawford, *thin solid films*, 1970, **5**, 187.

23. X. H. Huang, L. Li, X. Luo, X. G. Zhu, and G. H. Li, J. Phys. Chem. C. 2008, 112, 1468.
24. Z. Zhao, H. Wang, B. Wang, J. G. Hou, G. L. Liu, and X. F. Jin, *Phys. Rev. B*, 2002, **65,** 235413.
25. W. L. O'Brien and B. P. Tonner, *Phys. Rev. B*, 1994, **50**, 2963.
26. R. Nakajima, J. St¨ohr, and Y. U. Idzerda, *Phys. Rev. B.*,1999, **59**, 6421.

